ONLINE REPOSITORY

ORAI1 mutations abolishing store-operated Ca^{2+} entry cause a new form of anhidrotic ectodermal dysplasia with immunodeficiency (EDA-ID)

Jayson Lian (B.A.)[1,†], Mario Cuk (M.D., Ph.D.)[2,†], Sascha Kahlfuss (M.D.)[1,†], Lina Kozhaya (Ph.D.)[3], Martin Vaeth (Ph.D.)[1], Frédéric Rieux-Laucat (Ph.D.)[4,5], Capucine Picard (M.D., Ph.D.)[5,6], Melina J. Benson (B.A.)[1], Antonia Jakovcevic (M.D.)[7], Karmen Bilic (M.D.)[8], Iva Martinac (M.D.)[2], Peter Stathopulos (Ph.D.)[9], Imre Kacskovics (M.D.)[10], Thomas Vraetz (M.D.)[11], Carsten Speckmann (M.D.)[11,12], Stephan Ehl (M.D.)[11,12], Thomas Issekutz (M.D.)[11], Derya Unutmaz (M.D.)[3], and Stefan Feske (M.D.)[1]

Methods

Case reports

Patient 1 (P1)

P1 is the index patient (A-II-1 in **Fig. 1A**) of kindred A **(Tables 1 and E1, Fig. E1A).** The patient is a 13-year old male born to consanguineous parents of Nova Scotian origin. From two weeks of age he suffered from continuous rhinorrhea and prolonged rotavirus enteritis. He was diagnosed with a lobar pneumonia and was treated with antibiotics with some benefit at six months. He failed to thrive and had increased breathing difficulties suggestive of bronchiolitis at the time. Because of a lack of clinical improvement and abnormalities in immunoglobulins and lymphocyte subsets, a lung biopsy was performed, which showed an extensive *Pneumocystis jiroveci* infection. He was treated with trimethoprim-sulfamethoxazole and eventually responded with complete recovery. No signs of autoimmunity such as autoimmune hemolytic anemia (AIHA) or thrombocytopenia were apparent. A relative of the P1 (the daughter of his maternal grandfather's brother) had died of *Pneumocystis jiroveci* pneumonia (PCP) at ~ 3 years of age 40 years ago and had been diagnosed with Nezelof syndrome, which was associated with reduced T cell proliferation.

The immunological analysis of P1 at 7 months showed a normal white blood cell count including normal absolute lymphocyte numbers and lymphocyte subsets **(Table E1)**. His $CD4^+$ T

cells were 95% $CD45RO^+$ and 5% $CD45RA^+$ indicating a paucity of naïve $CD4^+$ T cells. His B cells were 68% IgD^+, 8% IgM^+, 4% IgG^+ and 20% IgA^+ at the cell surface. P1 showed dysgammaglobulinemia with normal IgG, but increased IgM and IgA levels. Immuno-electrophoresis showed oligoclonal IgA and increased lambda chains. No specific antibodies to immunizations with diphtheria, tetanus and pneumococcus were detectable. Lymphocyte proliferation studies showed essentially no response to mitogens (PHA, Con A, PWM, anti-CD3), antigens (*Staphylococcus aureus*, tetanus toxoid, diphtheria toxoid, *Candida albicans*), and mixed lymphocyte cultures **(Table E1)**. Because of his severely impaired T cell function and infections, P1 was treated at 13 months of age with a matched HSCT from an unrelated donor, which engrafted well and was complicated only by mild episodes of graft-versus-host disease (GvHD) that were treated with cyclosporine and steroids. At 13 years of age, he is in immunologic remission with normal T and B cell numbers, a diverse TCR Vβ repertoire, normal T cell proliferation to mitogens, antigens and in mixed lymphocyte cultures. His serum immunoglobulin levels are normal and he responded well to both protein and polysaccharide antigens (except for hepatitis B), as well as live virus vaccines.

In addition to CID, P1 suffers from congenital muscular hypotonia. As an infant, he was floppy and showed delayed sitting and walking with discernable gait problems, which was initially thought to be related to his chronic illness and later ascribed to a steroid myopathy. Detailed muscular assessment at ~ 3.5 years of age showed reasonable strength in his upper extremities, but considerable weakness of his facial muscles and a positive Gower's sign. His fine motor development was normal. He had right eye esotropia which was treated by surgery. Electromyography and nerve conduction studies performed at the time were normal. A muscle biopsy of the right gastrocnemius muscle followed by ATPase staining showed an almost complete absence of type 2 muscle fibers (**Fig. E2D**). No evidence of inflammatory muscle changes was found. P1's myophathy continues to slowly worsen and at 6 years of age, he began to use a wheel chair intermittently especially at school. P1 shows symptoms of anhidrotic ectodermal dysplasia. He has mild hypothrichosis and produces very little sweat in response to iontophoresis despite normal appearing sweat glands in a skin biopsy taken at the age of 9 years (**Fig. E3B**)[1]. His dental development at 8 months showed pitted enamel hypoplasia and hypomineralization of incisors. He developed multiple dental abscesses and six of his permanent teeth have been extracted and virtually all other teeth had to be capped. P1 also has mild hypotrichosis. At 3 and 4 years of age, the patient fractured his tibia and his humerus, respectively, after minor falls. His bone mineral density at age of 4 years was significantly below normal. He is very bright intellectually and no cognitive deficits have been observed.

Patient 2 (P2)

P2 is the index patient (B-II-1 in **Fig. 1C**) of kindred B (**Table 1** and **E1, Fig. E1B**). She was born at term to unrelated parents and has one healthy sister. P2 presented acutely at age of 2 months with irritability, opisthotonus, tachycardia, tachypnea, hyperpyrexia, vomiting, diarrhea and dehydration. A chest X-ray showed bilateral lung infiltrates and her CSF contained 176 cells. Because of her meningitis, pneumonia and gastroenteritis of unresolved etiology, an empiric antimicrobial treatment regimen was started, which improved her condition at that time. At 3.5 months of age, P2 deteriorated severely due to *Klebsiella* and *Candida* sepsis, massive bilateral pneumonia (caused by *S. aureus*), pneumonitis (210,000 copies of CMV DNA/ml of BAL). She was treated with various antibiotics but without lasting results. At age of 6 months, P2 suffered from sepsis due to *Enterococcus cloacae* and *C. albicans* resulting in a life-threatening condition with disturbed consciousness, tachycardia, tachypnea and poor capillary perfusion. From age 6 months of age, P2 suffered from several life-threatening infections caused by respiratory syncytial virus (RSV), Norovirus, *Salmonella enteritidis*, *C. albicans*, *K. pneumoniae* and *S. aureus*, which resulted in progressively deteriorating respiratory function and acute respiratory distress syndrome (ARDS), pulmonary fibrosis and pulmonary hypertension necessitating mechanical ventilation. Despite intensive care, P2 died at 7.5 months of age from various infections including disseminated CMV and gram-negative cocci. The immunological analysis of P2 at 4 months of age showed normal total lymphocyte counts and numbers of B cells, but an increased CD4:CD8 T cell ratio **(Table1** and **Table E1**). Intracellular cytokine staining of $CD8^+$ T cells demonstrated undetectable IFN-γ production on two occasions. By contrast, tests for phagocytosis, respiratory burst and NK cells activity were normal. P2 had hyper- and dysgammaglobulinemia (IgG 25 g/L, IgE 666 kIU/L, IgA 3.53 g/L, IgM 1.66 g/L) **(Table E1)**. Her anti-CMV IgM serology at 6 months was negative, but positive for CMV DNA detected by PCR in plasma (246, 000 copies of CMV DNA/ml) and BAL (221,000 copies of CMV DNA/ml). When P2 first presented at 2 months of age, she appeared pale and was anemic (hematocrit 0.23; hemoglobin 75 g/L) and received blood transfusions to correct her anemia. In addition, she was thrombocytopenic and leukopenic at 7 months of age. Throughout her life, P2 presented with moderate hepatosplenomegaly as well as cervical and inguinal lymphadenopathy. In addition to CID, P2 suffered from congenital muscular hypotonia, muscular hypotrophy and failure to thrive. She was sluggish with poor head control, hyperextensive, lacked spontaneous movements and facial mimicking. Her muscular hypotonia mostly affected facial, axial and respiratory musculature contributing to her respiratory failure. She had mydriasis with very slow pupil reactions to direct light. A biopsy from the deltoid muscle at 6

months of age showed variable fiber size but otherwise normally structured fibers (**Fig. E2C**). Histochemical analysis of frozen sections showed normal PAS, Gomory trichrome and oil-red O staining. Stains for oxidative enzymes NADH, SDH, COX and menadione were normal and showed a mosaic pattern of type I and II muscle fibers. Electron microscopic (EM) analysis revealed accumulation of glycogen, increased number and size of the lipid droplets, swelling of the sarcoplasmic reticulum and myelin-like figures as unspecific sign of myopathy (**Fig. E2I-K**). EM further showed increased numbers of mitochondria appearing swollen and with dissolved cristae structure. P2 also showed symptoms of EDA. Her hair was sparse, thin, brittle and prone to fall off, whereas her nails looked normal. She was unable to sweat, resulting in dry and exfoliate skin.

Patients 3 and 4 (P3, P4)

P3 is the index patient (C-II-2 in **Fig. 1E**) of kindred C (**Table 1** and **E1**, **Fig. E1C**) and the younger brother of P4. He was born at term to unrelated parents. He first presented with acute RSV positive bronchiolitis at 10 days after birth. Given the CID and autoimmunity of his older sister, P3 was hospitalized at 1 month of age and initially managed in accordance with UK PIDNet standards of care for CID patients including protective isolation measures and opportunistic infections prevention. Nevertheless, he suffered from infections with a wide spectrum of pathogens including *Stenotrophomonas*, extended-spectrum β-lactamase (ESBL)-producing *K. pneumoniae*, *C. albicans* and *Aspergillus fumigatus*. P3 also developed persistent CMV infection (up to 20,000 copies of CMV DNA/ml of plasma) which was resistant to standard treatment with ganciclovir, but responded to treatment with foscarnet and CMV specific and nonspecific immunoglobulins (<1,000 copies of CMV DNA/ml of plasma). Because P3 had received BCG vaccination, he was provided with anti-mycobacterial treatment. His immunological analysis in the first months after birth revealed increased percentages of $CD4^+$ T cells (71%) but decreased numbers of naive $CD45RA^+$ $CD4^+$ T cells. His $CD8^+$ T cells (9%) and $CD19^+$ B cells were reduced **(Table E1)**. His T cells showed poor or no proliferation following stimulation with mitogens (PHA, PMA/ionomycin) and anti-CD3 (OKT3), respectively **(Table E1)**. Serum immunoglobulins were strongly elevated, in particular IgE. At 3 months of age, P3 was diagnosed with Coombs positive AIHA. Besides autoantibodies against erythrocytes, he was tested positive for anti-cardiolipin antibodies (ACI IgG 12 GPL U/ml), ANAs and ANCAs.

In addition to CID, P3 suffered from congenital, non-progressive muscular hypotonia involving the facial, respiratory and axial musculature. Muscular hypotonia manifested with poor head control, diminished motor activity and overall delayed motor development **(Fig. E2A)**. P3

had mydriasis, bilateral partial iris hypoplasia **(Fig. E2B)** and showed slow pupillary light reflexes. H&E stains of a quadriceps muscle biopsy at 2.5 months showed normally structured fibers (not shown). Histochemical analysis of frozen sections showed normal PAS, Gomory trichrome and oil-red O staining. Stains for oxidative enzymes NADH, SDH, COX and menadione were normal and showed a mosaic pattern of type I and II muscle fibers. EM showed increased numbers of mitochondria appearing swollen and with dissolved cristae structure; in addition, signs of mitophagy were present (**Fig. E2E-H**). A mitochondrial respiratory chain enzyme analysis in skeletal muscle showed normal results. Furthermore, P3 showed symptoms of anhidrotic ectodermal dysplasia. His skin was very dry and exfoliate, his hair was sparse, thin and brittle (**Fig. E3D**). A sweat test using pilocarpin iontophoresis confirmed the diagnosis of anhidrosis. At 3 months of age, P3 experienced several attacks of facial flashing accompanied with tachycardia, tachypnea and hypertension (similar to his sister P4), potentially due to his inability to sweat and heat intolerance. The teeth of P3 showed severely cracked and chipped enamel and loss of cuspal enamel with exposure of underlying dentine (yellow). The visible discoloration, the excessive wear and loss of enamel in the teeth indicate a developmental defect consistent with the diagnosis hypocalcified amelogenesis imperfecta (type III) (**Fig. E3C**). Because of his CID and that of his older sister P4, P3 was treated by HSCT at 7 months of age with a HLA-matched donor.

P4 (C-II-1 in **Fig. 1E, Table 1 and E1**, **Fig. E1C**) is the older sister of P3. She was born at term but failed to thrive and from ~3.5 months of age, she suffered from frequent, severe and prolonged upper and lower respiratory tract infections (bronchiolitis, pneumonia and pneumonitis) caused by a large spectrum of bacteria (mostly *P. aeruginosa*, *S. aureus*, *K. pneumoniae*), fungi (*A. fumigatus, C. albicans*) and viruses (RSV, CMV, Adenovirus, Influenza, Parainfluenza). Repeated episodes of gastroenteritis were due to Adenovirus or Rotavirus infections. During her first year, P4 developed disseminated and chronic CMV infection with ~ 2,670,000 copies of CMV DNA/ml plasma despite yearlong treatment with ganciclovir, foscarnet and anti-CMV specific immunoglobulins. A lung biopsy showed severe CMV pneumonitis (**Fig. E3A**) At 6.5 months, she developed BCGitis after BCG vaccination and was treated with tuberculostatics for several months. In her second year, her respiratory failure became more pronounced necessitating mechanical ventilation and intensive care management on several occasions. She continued to suffer from multiple infections including with *E. faecalis, A. baumani, P. aeruginosa, S. aureus, K. pneumonie* and disseminated CMV infection at 16 months, causing pneumonitis, chorioretinitis with blindness, colitis and encephalitis.

From 7 months onwards, P4 developed autoimmunity with several life-threatening episodes of AIHA (Hb 4 g/dL, Hkt 0.1). In her second year, P4 had several severe episodes of acute bleeding from the GI tract due to autoimmune thrombocytopenia resulting in circulatory shock. In addition, she was diagnosed with autoimmune neutropenia and anti-phospholipid syndrome with elevated levels of anti-beta 2-GPI (52 GPL U/ml) and anti-cardiolipin antibodies (ACl-IgG 121 GPL U/ml, ACl-IgM 25 GPL U/ml). She also tested positive for direct and indirect Coombs tests and anti-platelet antibodies. The immunological analysis of P4 at 4.5 months of age showed an abnormal CD4/CD8 ratio with a significant increase of $CD4^+$ and decrease of $CD8^+$ T cells **(Table E1)**. Flow cytometric analysis of cytokine levels showed very low IFN-γ production by $CD8^+$ T cells after PMA and ionomycin stimulation on three occasions. P4 also had hypergammaglobulinemia (IgG 25 g/L, IgE of 7169 kIU/L).

In addition to CID, P4 suffered from congenital muscular hypotonia with delayed motor development. She was sluggish from birth with very poor head control, diminished motor activity and worm-like movements. Her marked muscular hypotonia mostly affected facial, axial and respiratory musculature with a tendency to develop intermittent respiratory failure. She had mydriasis with unresponsive pupils and rotatory nystagmus. H&E stains of deltoid muscle biopsy at 6 months of age showed variable size of muscle fibers but otherwise normally structured fibers. Histochemical analysis of frozen sections showed normal PAS, Gomory trichrome and oil-red O staining. Stains for oxidative enzymes NADH, SDH, COX and menadione were normal and showed a mosaic pattern of type I and II muscle fibers. EM of the same muscle biopsy showed increased numbers and size of the lipid droplets but no specific mitochondrial abnormalities. The activity of respiratory chain complexes I and IV was reduced (complex I: 0.048 U per unit citrate synthase (UCS) [normal range 0.17-0.56] and 3.0 U per gram non-collagen protein (gNCP) [normal range 15.8-42.8]; complex IV 0.862 U/UCS [normal range 1.1-5] and 53.6 U/gNCP [normal range 112-351]), wheres complex II/III function was normal (0.2 U/UCS [normal range 0.08-0.45]) as reported in [2], suggesting a mitochondrial etiology of her myopathy. Sequencing of mitochondrial (mt) DNA for mutations of tRNA genes was normal and mtDNA depletion was excluded by real-time PCR. Urine organic acid analysis revealed elevated levels of ethylmalonic and glutaric acid as observed in some mitochondriopathies. P4 also showed symptoms of EDA. Her teeth at 10 months of age showed yellowish discoloration. Her skin was very dry and exfoliate, and her hair was sparse, thin, fragile and brittle. A sweat pilocarpine sweat test confirmed the diagnosis of anhidrosis. After 6 months, her anhidrosis resulted in thermoregulatory instability, attacks of facial blushing, hypertension, tachycardia (up to 200-250/min) and tachypnea (up to

100/min). P4 died at 2.5 years of age due to multiple infections including disseminated CMV infection and respiratory failure.

Patient 6 (P6)

P6 has been reported previously [3-5]. He is homozygous for a ORAI1 p.R91W missense mutation that abolishes SOCE. Clinically, P6 suffered from CRAC channelopathy with CID, autoimmunity, muscular hypotonia and EDA (**Table 1, Table E1, Table E2**)[6]. At 4 months of age, he received a HSCT to cure his CID, which resulted in mixed chimerism with the presence of both donor and recipient cells in his PBMC. When P6 was reevaluated for chimerism of his PBMC at 15 years of age, no donor NK cells and only 5-15% donor T and B cells were detectable by short tandem repeat (STR) analysis[7]. At 19 years of age, repeat testing of his PBMC showed complete autologous reconstitution of his granulocyte compartment and complete lack of SOCE in his $CD4^+$ and $CD8^+$ T cells [8, 9] indicating that all T cells in the 19-year-old P6 were autologous and not of HSCT donor origin. PBMC were isolated from P6 at 20 years of age before he received a second HSCT (to prevent a recurrence of his CID) and used for this study.

DNA sequencing analyses

Genomic DNA was extracted from cells using the Flexigene DNA Kit (QIAGEN, Hilden, Germany). PCR was conducted using the following primers flanking exons 1 and 2 of the ORAI1 gene: fwd 5'ACAACAACGCCCACTTCTTGGTGG and rev 5'TGCTCACGTCCAGCACCTC (exon 1); fwd 5'TCTTGCTTTCTGTAGGGCTTTCTG and rev 5'TCTCAAAGGAGCTGGAAGTGC (exon 2). PCR products were separated on 1.5% agarose gels, excised using the QIAGEN gel extraction kit and sequenced directly (Genewiz Inc., South Plainfield, NJ) using the following primers: fwd 5'AGCATGCAAAACAGCCCAGG and rev 5'ACGGTTTCTCCCAGCTCTTC (exon 1); fwd 5'TGACAGGAGGAGAGCTAGG and rev 5'AAGAGATCCTCCTGCCTTGG (exon 2). Sequence alignments were performed using T-Coffee software (Swiss Institute of Bioinformatics, http://tcoffee.vital-it.ch/cgi-bin/Tcoffee_cgi/index.cgi) and sequence traces were visualized using Sequence Scanner version 1.0. CADD scores were calculated using combined annotation dependent depletion analysis available on the the Mutation Significance Cutoff (MSC) Server http://pec630.rockefeller.edu:8080/MSC/

Synthesis of cDNA and quantitative real-time PCR

Total RNA was extracted from T cells and fibroblasts using Trizol Reagent (Invitrogen, Carlsbad, CA). cDNA was synthesized using Superscript IITM RT (Invitrogen, Carlsbad, CA) according to the manufacturer's instructions. Real-time PCR was performed using the iCycler system (BioRad Laboratories, Hercules, CA), SYBR green PCR kit (Applied Biosystems, Foster City, CA) and the following primers: fwd 5'TCAACGAGCACTCCATGCAG and rev 5'GGACGCTGACCACGACTA (ORAI1), fwd 5'CGCTCTCTGCTCCTCCTGTT and rev 5'CCATGGTGTCTGAGCGATGT (GAPDH). ORAI1 mRNA expression was normalized to GAPDH and calculated using the $2^{-\Delta C}{}_T$ method using the formula $2^{-(C_T(ORAI1) - C_T(GAPDH)}$.

Plasmids and retroviral transduction

Bicistronic retroviral vectors containing the coding sequences of wildtype ORAI1 or STIM1 and an IRES-GFP sequence have been described 9. Retroviral supernatants were generated by transfecting HEK293 cells with STIM1, ORAI1 or empty vectors as well as gag-pol and VSV-G packaging plasmids (Addgene). Two days later, viral supernatants were harvested and used for transduction of patient and control fibroblasts. After removal of cell debris by centrifugation, the viral supernatant supplemented with 6 µg/ml polybrene was added directly to fibroblasts for 8 hours. The transduction efficiency was evaluated by GFP expression.

Time-lapse Ca^{2+} imaging

Patient and HD control fibroblasts were seeded on sterilized 15 mm glass cover slips overnight and loaded for 45 minutes at room temperature with 3 µM Fura-2 AM (Invitrogen) in RPMI 1640 medium containing 10% FCS, 1% L-glutamate, 1% HEPES, and 1% Penicillin/Streptomycin before mounting in a RC20 flow chamber (Warner Instruments). T cells were loaded with 1 µM Fura-2 AM and attached to cover slips with poly-L-lysine. Fibroblasts and T cells were perfused with Ringer solution (155 mM NaCl, 4.5 mM KCl, 1-2 mM $CaCl_2$, 1 mM $MgCl_2$, 10 mM D-glucose, and 5 mM Na-Hepes, pH 7.4). Ca^{2+}-free Ringer solution was prepared by substituting 2 mM $MgCl_2$ for $CaCl_2$. Cells were stimulated with thapsigargin (1 µM, EMD Biosciences, San Diego, CA) to deplete intracellular Ca^{2+} stores. Fura-2 emission was detected at 510 nm following excitation at 340 and 380 nm using an Olympus IX81 inverted epifluorescence microscope and SlideBook imaging software v4.2 (Olympus). Fura-2 emission ratios (340 nm /380 nm) were calculated every 5 s interval after background subtraction. For each experiment, 20-100 cells were analyzed. Ca^{2+} influx rates were inferred from the maximal rate of the initial rise of Fura-2 emission ratios in the first 15 s after Ca^{2+} re-addition.

Modeling of human ORAI1 structure and mutations

Homology models of the human ORAI1 protein structure were generated based on the Drosophila melanogaster Orai crystal structure (4HKR.pdb) as a template using the MODELLER software (version 9.16) [10]. First, the human dimer unit was modeled using the fly:human sequence alignment as reported before [11]. Subsequently, the ORAI1 hexamer was assembled by backbone atom superposition of the modeled human dimer with each of the fly dimer units. G98R and L194P mutations found in human patients were modeled using a similar approach after the respective sequence modifications. These models orient the mutant side chains in positions which are homologous to the wildtype residues and do not show the precise structural consequences of the substitutions which requires new high resolution structural data.

References

1. Concepcion AR, Vaeth M, Wagner LE, Eckstein M, Hecht L, Yang J, et al. Store-operated Ca2+ entry regulates Ca2+-activated chloride channels and eccrine sweat gland function. Journal of Clinical Investigation 2016; 126:4303-18.

2. Maus M, Cuk M, Patel B, Lian J, Ouimet M, Kaufmann U, et al. Store-Operated Ca2+ Entry Controls Induction of Lipolysis and the Transcriptional Reprogramming to Lipid Metabolism. Cell Metabolism 2017; 25:698-712.

3. Feske S, Gwack Y, Prakriya M, Srikanth S, Puppel SH, Tanasa B, et al. A mutation in Orai1 causes immune deficiency by abrogating CRAC channel function. Nature 2006; 441:179-85.

4. Feske S, Draeger R, Peter HH, Eichmann K, Rao A. The duration of nuclear residence of NFAT determines the pattern of cytokine expression in human SCID T cells. J Immunol 2000; 165:297-305.

5. Feske S, Muller JM, Graf D, Kroczek RA, Drager R, Niemeyer C, et al. Severe combined immunodeficiency due to defective binding of the nuclear factor of activated T cells in T lymphocytes of two male siblings. Eur J Immunol 1996; 26:2119-26.

6. Lacruz RS, Feske S. Diseases caused by mutations in ORAI1 and STIM1. Ann N Y Acad Sci 2015; 1356:45-79.

7. Maul-Pavicic A, Chiang SC, Rensing-Ehl A, Jessen B, Fauriat C, Wood SM, et al. ORAI1-mediated calcium influx is required for human cytotoxic lymphocyte degranulation and target cell lysis. Proceedings of the National Academy of Sciences of the United States of America 2011; 108:3324-9.

8. Elling R, Keller B, Weidinger C, Haffner M, Deshmukh SD, Zee I, et al. Preserved effector functions of human ORAI1- and STIM1-deficient neutrophils. J Allergy Clin Immunol 2016; 137:1587-91 e7.

9. Desvignes L, Weidinger C, Shaw P, Vaeth M, Ribierre T, Liu M, et al. STIM1 controls T cell-mediated immune regulation and inflammation in chronic infection. J Clin Invest 2015.

10. Webb B, Sali A. Comparative Protein Structure Modeling Using MODELLER. Curr Protoc Bioinformatics 2014; 47:5 6 1-32.

11. Hou X, Pedi L, Diver MM, Long SB. Crystal structure of the calcium release-activated calcium channel Orai. Science 2012; 338:1308-13.

12. Byun M, Abhyankar A, Lelarge V, Plancoulaine S, Palanduz A, Telhan L, et al. Whole-exome sequencing-based discovery of STIM1 deficiency in a child with fatal classic Kaposi sarcoma. J Exp Med 2010; 207:2307-12.

13. Le Deist F, Hivroz C, Partiseti M, Thomas C, Buc HA, Oleastro M, et al. A primary T-cell immunodeficiency associated with defective transmembrane calcium influx. Blood 1995; 85:1053-62.

14. Parry DA, Holmes TD, Gamper N, El-Sayed W, Hettiarachchi NT, Ahmed M, et al. A homozygous STIM1 mutation impairs store-operated calcium entry and natural killer cell effector function without clinical immunodeficiency. J Allergy Clin Immunol 2016; 137:955-7 e8.

15. Partiseti M, Le Deist F, Hivroz C, Fischer A, Korn H, Choquet D. The calcium current activated by T cell receptor and store depletion in human lymphocytes is absent in a primary immunodeficiency. J Biol Chem 1994; 269:32327-35.

16. Wang S, Choi M, Richardson AS, Reid BM, Seymen F, Yildirim M, et al. STIM1 and SLC24A4 Are Critical for Enamel Maturation. J Dent Res 2014; 93:94S-100S.

17. Maus M, Jairaman A, Stathopulos PB, Muik M, Fahrner M, Weidinger C, et al. Missense mutation in immunodeficient patients shows the multifunctional roles of coiled-coil domain 3 (CC3) in STIM1 activation. Proc Natl Acad Sci U S A 2015; 112:6206-11.

18. Dahmane R, Djordjevic S, Simunic B, Valencic V. Spatial fiber type distribution in normal human muscle Histochemical and tensiomyographical evaluation. J Biomech 2005; 38:2451-9.

Supplementary Figures

Figure E1: Genomic DNA sequences of patients from 3 unrelated kindreds with autosomal recessive *ORAI1* mutations. A, Kindred A. The index patient P1 (A-II-1) is homozygous for a del541C mutation in exon 2 of *ORAI1* that results in a truncated ORAI1 p.V181SfsX8 protein. His

healthy parents are heterozygous for the same mutation. **B,** Kindred B. The index patient P2 (B-II-1) is homozygous for a n.T581C transition in exon 2 of *ORAI1* that results in a mutant ORAI1 p.L194P protein. Her healthy sister and parents are heterozygous for the same mutation. **C,** Kindred C. The index patient P3 (C-II-2) and his sister P4 (C-II-1) are homozygous for a n.G292C transversion in exon 1 of *ORAI1* that results in a mutant ORAI1 p.G98R protein. His healthy brother and parents are heterozygous for the same mutation.

Figure E2: Histological and clinical findings in ORAI1 deficient patients related to their muscular hypotonia. A, Poor head control of P3 at ~ 3 months of age. **B,** Partial iris hypoplasia in P3 at 3 months of age. **C,** H&E stain of muscle fibers of P2 shows no abnormalities. Magnification 40x. **D,** ATPase stain of a biopsy of the right gastrocnemius muscle of P1 at 5 years of age shows a predominance of type 1 muscle fibers (I, black arrowhead) and an almost complete absence of type 2 muscle fibers (II, yellow arrowhead). The normal frequency of Type 1 fibers in gastrocnemius muscle is 54-63% [18]. **E-L,** Electron microscopy of muscle biopsies of P2 (E-J) and P3 (K, L). Cross sections show several tight, round myofibrils and signs of mitochondrial damage. Mitochondria in some muscle fibers appear swollen with dissolved cristae structure (E, H-J) compared to other fibers with healthy-looking mitochondria (E, G). Autophagic vacuoles with mitochondrial cargo (K, L). Panels G-J are enlarged areas from E and F indicated by yellow boxes; panels K, L are from additional regions. Magnification 20,000x (E, G, H, K, L), 40,000x (F, I, J).

Figure E3: Histological and clinical findings in ORAI1 deficient patients related to their EDA and immunodeficiency. A, H&E stain of a lung biopsy from P4 shows CMV pneumonitis with characteristic large cells that have a prominent basophilic nuclear inclusion and halo (arrow). Magnification 100x. **B,** H&E stain of a skin biopsy of P1 at 1 year of age shows the presence of eccrine sweat glands in the dermis (arrows). **C,** Hypocalcified amelogenesis imperfecta (type III) in P3 at 6 years of age. Severely cracked and chipped enamel and loss of cuspal enamel with exposure of underlying dentine (yellow). The visible discoloration, the excessive wear and loss of enamel in the teeth indicate a developmental defect. **D**, Sparse, thin and brittle hair of P3 at 18 months of age.

Figure E4: Gating strategy to identify NK, iNKT and γδ T cells. PBMCs from P6 and a HD control were stained with antibodies against CD3, HLA-DR, CD4, CD8, CD16, CD56, the invariant

TCR Vα24Jα18 chain and the γδTCR. $CD3^-$ $HLA\text{-}DR^-$ cells were further analyzed for different NK cell populations based on CD16 and CD56 expression. $CD3^+$ cells were analyzed for TCR $V\alpha24J\alpha18^+$ iNKT cells. $CD3^+$ cells were further analyzed for $CD4^+$ and $CD8^+$ T cells. $CD4^-CD8^+$ and $CD4^-CD8^-$ (double negative, DN) cells were analyzed for γδ TCR^{dim} and γδ TCR^{high} cells.

Patient	**P1** (A-II-1)	**P2** (B-II-1)	**P3** (C-II-2)	P4 (C-II-1)	P5*	P6*
***ORAI1* mutation**	V181SfsX8	L194P	G98R	G98R	R91W	R91W
Age at analysis	7 months	4 months	6 months	4.5 months	5 months	1 month
Lymphocytes (/µl)	5920	normal	9800		9600	6800
T cells (%)						
$CD3^+$	59 [49-76]		**82** [49-76]	**82** [54-80]	**85** [51-77]	75 [60-85]
$CD4^+$	44 [31-56]	**high**	**71** [31-56]	**79** [25-46]	**70** [35-56]	46 [41-68]
$CD8^+$	14 [12-24]	**low**	**9** [12-24]	**9** [15-42]	**11** [12-23]	**24** [9-23]
$CD45RO^+$ $CD4^+$	**95** [5-12]		**92** [5-12]			
$CD45RA^+$ $CD4^+$	**5** [88-95]		**8** [88-95]		**71** [77-94]	**73** [77-94]
B cells (%)						
$CD19^+$ or $B220^+$	25 [14-37]	normal	**8** [14-37]	**9** [9-37]	**12** [15-32]	**2** [15-32]
NK cells (%)						
$CD16^+CD56^+$	5 [3-15]	**low**	7 [3-15]	6.2 [5-20]		
T cell proliferation (cpm)						
PHA	**1.9** [69.1±4.8]		**32** [>50]		**33** [80]	**27.2** [71.2]
ConA	**2.2** [38.7±3.1]				**5** [68]	**11.4** [50.5]
Pokeweed-mitogen	**2.5** [32.4±3.7]					
OKT3	**0.7** [62.6±4.3]		**0.3** [>30]		**0.9** [130]	**11.6** [45.4]
OKT3+CD28						**1** [31]
PMA 10^{-7}M+Ionomycin10^{-5}M			**29** [>80]		**0.04** [3]	**1** [30]
S. aureus	**0.9** [4.3±0.7]					
Tetanus toxoid	**0.5** [39.7±7.6]					
Diphteria toxoid	**0.6** [23.5±5.3]					
Candida albicans	**1.4** [35.9±6.5]					
Mixed lymphocyte culture	**2.5** [16.5±2.7]					
Antibodies (serum)						
IgM (g/L)	**Increased**	**1.66** [0.26-0.96]	**1.24** [0.34-0.95]		**1.6** [0.3-0.9]	0.5 [0.3-0.9]
IgG (g/L)	normal	**25.00** [1.88-5.36]	21.36** [2.4-4.4]	**25.00** [1.88-5.36]	**11.4** [2.3-5.5]	**6.6** [2.3-5.5]
IgA (g/L)	**6.01** [0.08-0.54]	**3.53** [0.04-0.72]	**1.15** [0.2-0.62]		**7.0** [0.1-0.6]	**1.8** [0.1-0.6]
IgE		**666 g/L**	**>5000 KUl/l**	**7169 g/L**		
Seroconversion	**none**	**none**	**none**	**none**	**none**	**none**

Table E1: Immune cell populations and function of novel P1-P4.

[ ] indicate normal values for the indicated age and analyzing laboratory. For T cell proliferation data, [ ] indicates cpm of T cells from healthy donor day controls. Numbers in bold indicate abnormal values.

Abbreviations: cpm, counts per minute; Ig, Immunoglobulin; n.d., not determined

* as published in McCarl et al., 2009

** after IVIgG infusion

Gene	Mutation	Anhidrotic ectodermal dysplasia (EDA)				Immunodeficiency (ID)	References
		Anhidrosis		Dental enamel defect	Skin and hair		
		Clinical	Test				
ORAI1	**p.V181SfsX8** (P1)	Y	Y	Y	Hypotrichosis	Y	this study
	p.L194P (P2)	Y	Y	*	Hypotrichosis	Y	this study
	p.G98R (P3)	Y	Y	Y**	Hypotrichosis	Y	this study
	p.G98R (P4)	Y	Y	Y	Hypotrichosis	Y	this study
	p.R91W	n.r.	n.r.	n.r.*	n.r.	Y	Feske et al. (1996); Feske et al. (2006)
	p.R91W (P6)	Y	Y	Y**	N	Y[§]	Feske et al. (2000); Feske et al. (2006)
	p.A88SfsX25	Y	Y	n.r.*	N	Y	Partiseti et al. (1994); McCarl et al. (2009)
	p.A103E/p.L194P	Y	Y	Y**	N	Y	Le Deist et al. (1995); McCarl et al. (2009)
	p.H165PfsX1	n.r.	n.t.	n.r.*	N	Y	Chou et al. (2015)
	p.R270X	n.r.	n.t.	n.r.*	N	Y	Badran et al. (2016)
STIM1	p.E128RfsX9	n.r.	n.t.	Y	n.r.	Y	Picard et al. (2009)
	p.E128RfsX9	n.r.	n.t.	Y	n.r.	Y	Picard et al. (2009)
	C1538-1 G>A	n.r.	n.t.	n.r.	n.r.	Y	Byun et al. (2010)
	p.R429C	Y	Y	Y	n.r.	Y	Fuchs et al. (2012), Maus et al. (2015)
	p.R429C	Y	Y	Y	n.r.	Y	Fuchs et al. (2012), Maus et al. (2015)
	p.R426C	Y	Y	Y	n.r.	n.r.	Wang et al. (2014)
	p.P165Q	Y	n.t.	Y	n.r.	Y	Schaballie et al. (2015)
	p.P165Q	Y	Y	Y	n.r.	Y	Schaballie et al. (2015)
	p.L74P	Y	Y	Y**	n.r.	Y[#]	Parry et al. (2016)
	p.L74P	Y	Y[+]	Y**	n.r.	Y[#]	Parry et al. (2016)
	p.L374P	Y	Y[+]	Y	Hypotrichosis	Y[#]	*Unpublished*
	p.L374P	Y	Y[+]	n.r.	n.r.	Y[#]	*Unpublished*

Table E2: CRAC channelopathy causes anhidrotic ectodermal dysplasia with immunodeficiency (EDA-ID).

Shown in bold are *ORAI1* mutations reported in this paper.

Abbreviations: n.r., not reported; n.t., not tested; N, No; Y, Yes.

[#] Moderate Immunodeficiency

[§] Patient received a first curative HSCT at 4 months of age before onset of CID, and received a second HSCT after CMV pneumonia and loss of donor chimerism in his PBMC.

[+] Due to profound Hypohydrosis sweat test was not possible.

* Patient died before complete dentition.

** Hypocalcified amelogenesis imperfecta (type III)

Antigen	Manufacturer	Clone	Conjugation
CD3	Biolegend	SK7	APC-Cy7
CD3	Biolegend	UCHT1	Alexa700
CD4	Biolegend	OKT4	BV510
CD4	Biolegend	RPA-T4	PE
CD4	BioLegend	OKT4	Alexa700
CD8	Biolegend	HIT8a	Alexa700
CD8	Biolegend	RPA-T8	PE-Cy7
CD45RO	BD Pharmingen	UCHL1	PE-Cy7
CD45RO	Biolegend	UCHL1	APC-Cy7
CD57	Biolegend	HCD57	Pacific-Blue
CD16	Biolegend	3G8	Alexa488
CD56	Biolegend	HCD56	PerCP-Cy5.5
CD27	Biolegend	O323	PE-Cy7
CCR7	R&D	150503	FITC
HLA-DR	Biolegend	L243	APC-Cy7
Va24Ja18 TCR	Biolegend	6B11	APC
Foxp3	BioLegend	259D	PE
IL-2	Biolegend	MQ1-17H12	Alexa700
IL-22	eBioscience	22URTI	eF710
TNFα	Biolegend	MAb11	A488
γδ TCR +streptavidin	BD Biolegend	B1 -	biotinylated BV605
ViabDye	eBioscience	-	eF506

Table E3: Anti-human antibodies used for flow cytometry.

Figure E1

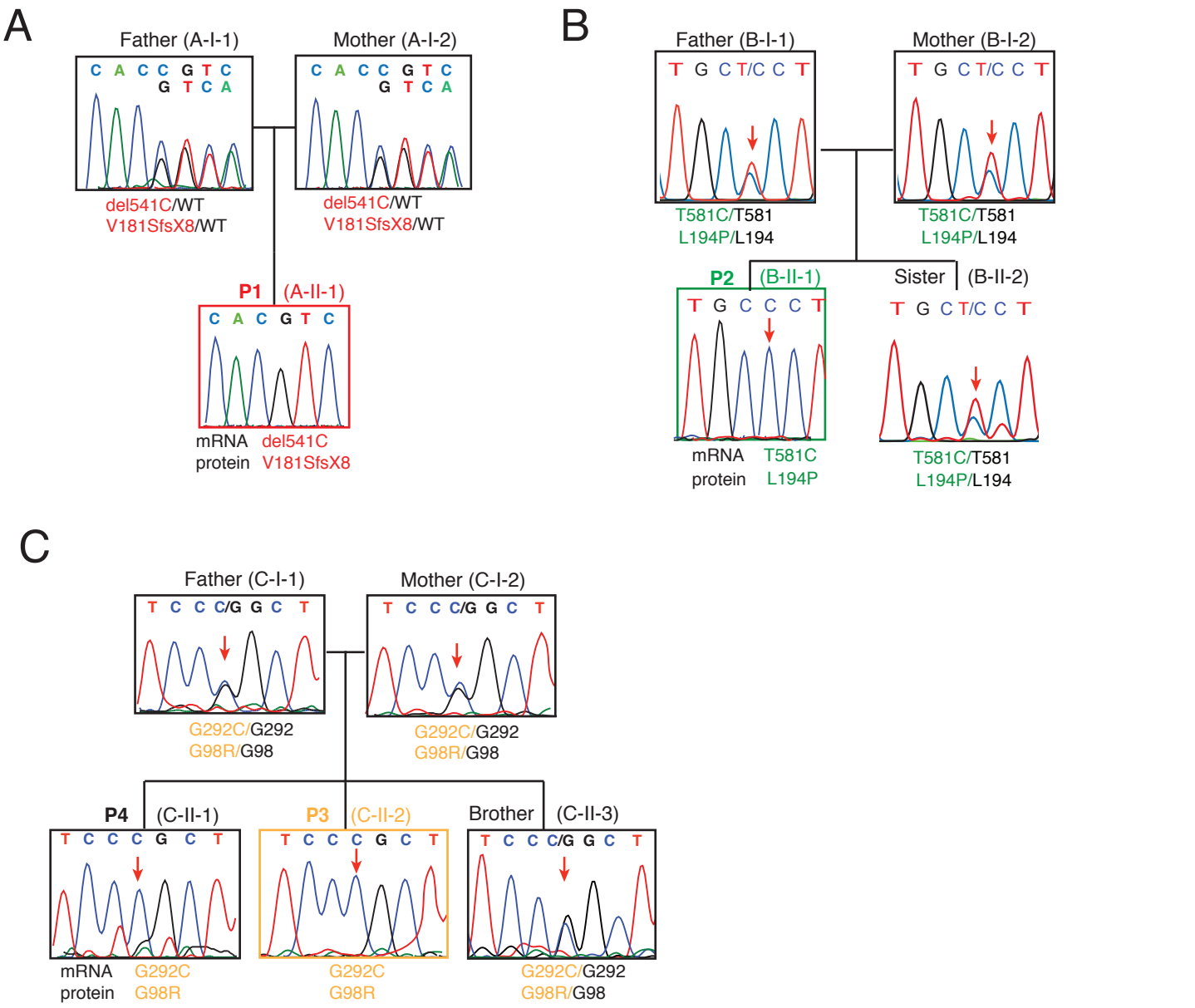
A
Father (A-I-1)
Mother (A-I-2)
del541C/WT
V181SfsX8/WT
del541C/WT
V181SfsX8/WT
P1 (A-II-1)
mRNA del541C
protein V181SfsX8
B
Father (B-I-1)
Mother (B-I-2)
T581C/T581
L194P/L194
T581C/T581
L194P/L194
P2 (B-II-1)
Sister (B-II-2)
mRNA T581C
protein L194P
T581C/T581
L194P/L194
C
Father (C-I-1)
Mother (C-I-2)
G292C/G292
G98R/G98
G292C/G292
G98R/G98
P4 (C-II-1)
P3 (C-II-2)
Brother (C-II-3)
mRNA G292C
protein G98R
G292C
G98R
G292C/G292
G98R/G98

Figure E2

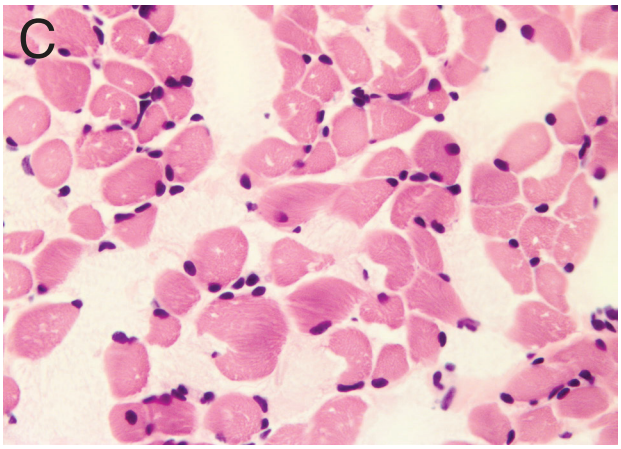

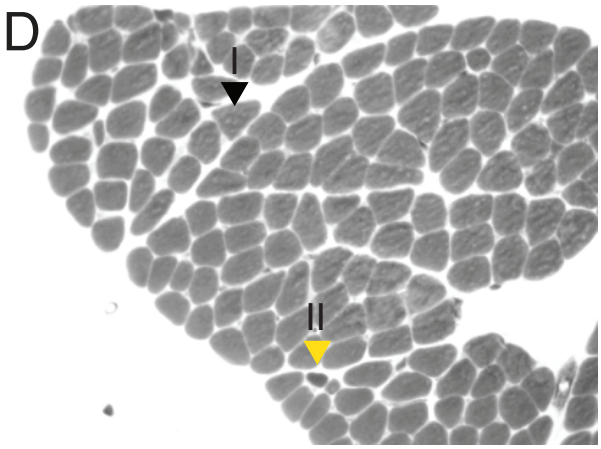

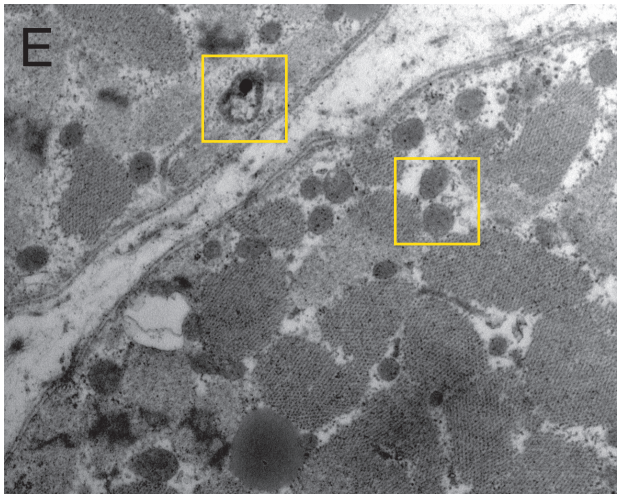

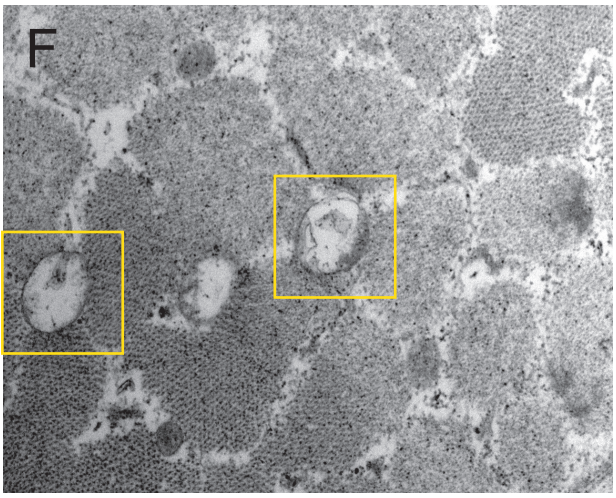

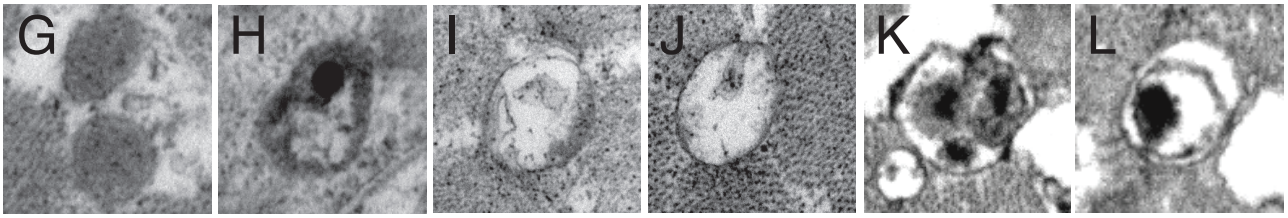

Figure E3

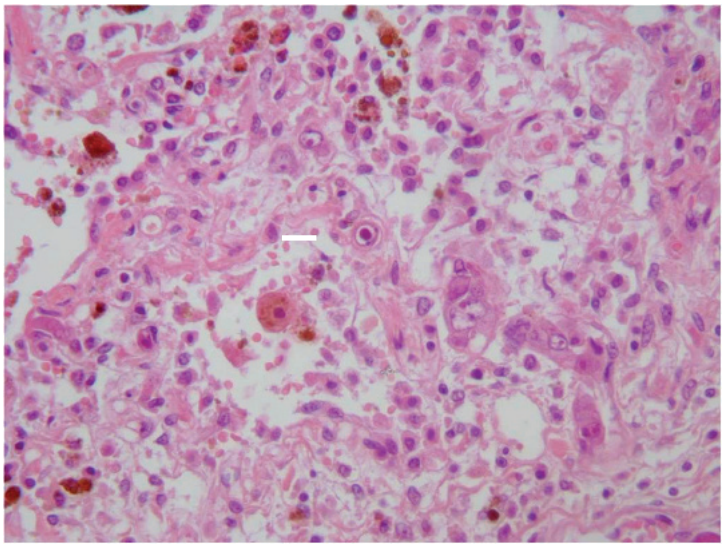

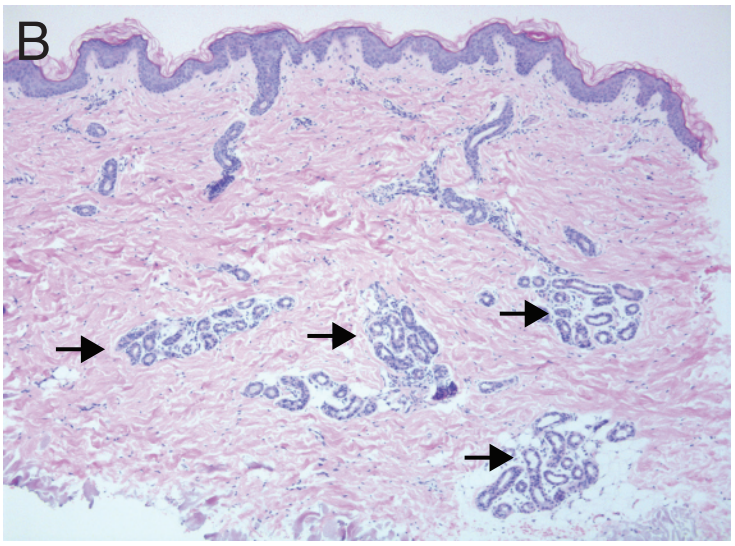

Figure E4

Gating strategy NK cells, iNKT cells and γδ T cells